*LA-UR-03-8314, Journal of Intelligent Material Systems and Structures, **15**(12), 941-953, 2004*

Improved Piezoelectric Self-Sensing Actuation

Garnett E. Simmers Jr., Jeffrey R. Hodgkins, David D. Mascarenas, Gyuhae Park[1], Hoon Sohn

Engineering Sciences & Application Division
Weapon Response Group
Los Alamos National Laboratory
Los Alamos, NM 87545

ABSTRACT

Self-sensing actuation allows a single piezoelectric element to be simultaneously used as both a sensor and actuator. A specially designed electric circuit, referred to as a bridge circuit, is required to realize the concept. However, precise equilibrium of the bridge circuit is extremely difficult to obtain because of continuous changes in environmental conditions. In this study, the effects of an unbalanced bridge circuit were analytically and experimentally evaluated in an attempt to quantify the variations in the piezoelectric capacitance in terms of performances in vibration testing and control. Once the dynamic characteristics of self-sensing actuation were identified and understood, methods for improving the system's performance are developed by utilizing capacitors in series and parallel with the piezoelectric patch. The analytical and experimental results clearly indicate that the new design scheme increases the stability of the system. However, the increase in stability comes at the cost of the increase in the power required for the control system.

[1] Author to whom correspondence should be addressed. E-mail: gpark@lanl.gov

NOMENCLATURE

C_p	Capacitance of a Piezoelectric self-sensing actuator
C_m, $C_{Matched}$	Matched capacitance
C_{add}	Added capacitance
C_{eq}	Equivalent capacitor
C_1	Signal conditioner capacitance
R_1	Signal conditioner resistance
V_s	Sensing voltage
V_p	Piezoelectric sensor Voltage
V_c	Control voltage
Z_{eq}	Signal conditioner impedance
Z_p	Impedance of Piezoelectric self-sensing actuator
Z_m	Matched capacitance impedance
K_{aad}, K_{aa}, K_{ss}	Actuator matrix gains
x1s	Sensor location 1
x2s	Sensor location 2
x1a	Actuator location 1
x2a	Actuator location 2
g	Positive position feedback (PPF) gain
w_{nf}	PPF natural frequency
z_{nf}	PPF damping ratio
ω	Natural frequency of system
ξ	Damping ratio of system

INTRODUCTION

When a single piezoelectric patch (PZT) is used as a self-sensing actuator, it possesses many advantages over the use of two separate PZT elements as individual sensors and actuators. The concept of a self-sensing actuator was first developed and published by Dosch et al (1992).[1] Self-sensing actuator systems are lighter and less costly than non-collocated sensor/actuator systems because they employ a single piezoelectric element. Furthermore, the collocation of sensing and actuation allows the control signal to be applied at the point of measured response, thereby eliminating the capacitive coupling between the sensor and actuator elements[1]. Goh and Coughley[2] presented results which demonstrate that, in the absence of finite actuator dynamics, structures controlled with collocated velocity feedback are unconditionally stable at all frequencies.

Subsequent to the work of Dosch et al[1], self-sensing piezoelectric actuators have been widely employed in vibration and control applications. Tzou and Hollkamp[3] investigated the use of self-sensing orthogonal modal actuators to effectively control vibration in beam-like structures. Frampton et al[4] and Dongi et al[5] investigated the feasibility of using a self-sensing actuator for active flutter suppression. Vallone[6] successfully applied self-sensing actuators to control vibrations in large-scale space structures. In addition, self-sensing actuation has been extended to active acoustic noise control[7,8] and structural health monitoring applications[9,10]. While most studies use monolithic piezoceramic material for its d_{31} coupling coefficients, Jones et al[11] applied the self-sensing actuation concept to PZT stack actuators used as a micropositioner. The authors used a nonlinear element in the self-sensing circuit to negate any nonlinear effects, thus improving the signal-to-noise ratio. Recently, Sodano et al[12] investigated

the feasibility of Macro-Fiber Composites used in self-sensing actuation for vibration reduction in flexible structures, such as inflatable space devices.

The advantages gained through the use of a piezoelectric self-sensing actuator are well-documented; however, some difficulties have limited the commercial acceptance of the self-sensing concept. First, the capacitance of PZT is temperature sensitive, causing it to vary significantly as temperature changes. When used as an actuator, the voltage applied to the piezoelectric material tends to be several times greater than the voltage generated during sensing. Since both signals occur simultaneously in the material, it becomes very difficult to distinguish the sensor voltage from the mixed signals, which is well summarized in Tani et al.[13] Bridge circuits, as shown in Figure 1, are the most popular way to separate the control and sensing signals, yet maintaining the balance of the bridge circuit present an even greater challenge. Most balanced bridge circuits use a "dummy" sensor to compensate for variations in environmental conditions such as temperature changes. The drawback of a self-sensing actuation circuit is the fact that there is no other PZT patch to act as a "dummy" sensor to counteract the changes in capacitance within the material caused by variations in temperature. Therefore, PZT used as self-sensing actuators can lead to control stability problems if the environmental conditions are not matched to the properties of the piezoelectric materials[13].

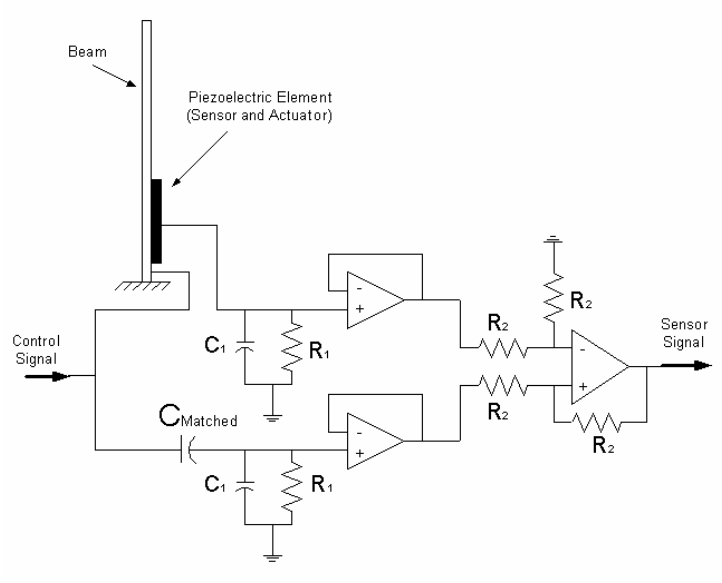

Figure 1: Self-sensing actuator with a bridge circuit[12]

As a consequence of its potential commercial value, the development of "robust" or "adaptive" self-sensing actuators became a recurrent research topic. Cole and Clark[14] and Vipperman and Clark[15] developed an adaptive filter algorithm to identify the feedthrough capacitance of the PZT to digitally compensate for parameter changes in self-sensing circuits. Oshima et al[16] designed μ-controllers to guarantee the robust performance in vibration suppression against the perturbations in the bridge is balance. Many researchers have cast the adaptive self-sensing actuation in the context of state-space observer-based problems. Spangler and Hall[17] firstly presented an observer-based approach for adaptive self-sensing coupled with the use of charge control to minimize the hysteretic effect of the PZT. Jones and Garcia[18] proposed a state estimation technique, referred to as Observer-Based Self Sensing (OBSS), which estimates the stress and strain state within as tructure by utilizing the piezoelectric constitutive relations with electric field and displacement information. Dong and Baoyuan[19] also implemented OBSS coupled with a compound circuit which integrates voltage driving and charge measuring components. Both OBSS methods use a generalized Maxwell Slip Hysteresis

model to compensate for the hysteretic effect of the PZT. Tonoli et al[20] developed a charge feedback amplifier to drive the PZT in self-sensing operation. The use of a charge feedback amplifier lowers the sensitivity to changes in the circuit parameters and reduces of the hysteresis compared to a voltage feedback amplifier. Okugawa and Sasaki[21] modeled the self-sensing system using system identification and state estimation approaches to increase stability. Nishigaki and Endo[22] use two PZT patches, with different thicknesses and areas but with equivalent capacitances. When installed on the surface of a structure, they can act as a "dummy" device to compensate for changes in temperature. The authors applied the technique for control of both a cantilever beam and a flexible circular ring. The possible interference or relative offset effects of the sensing voltages from two PZTs are not addressed in the paper, however.

To the authors' best knowledge, despite numerous studies in self-sensing actuation, quantitative assessment of the effects of unbalanced bridge circuits has never been established. Therefore, in this paper, the effects of the unbalanced bridge circuit are analytically and experimentally evaluated in an attempt to quantify the variations in the piezoelectric capacitance as a result of temperature changes. Once the dynamic characteristics of the circuit are identified, a new design scheme for PZT self-sensing actuation is proposed to minimize the effect of variations in PZT capacitance caused by temperature changes. The new design includes adding a capacitor in series or parallel with the PZT and matched capacitance. It has been found that the added capacitors increase the system stability with a slight decrease in the effectiveness of vibration reduction. Experiments were performed to validate the new design concept. Finally, future recommendations are summarized for more effective implementation of the new self-sensing design.

SELF-SENSING AND STRUCTURE MODELING

Bridge Circuit

In order to utilize a self-sensing piezoelectric actuator, it is necessary to separate the control voltage supplied to the PZT for actuation from the sensing voltage created by the material's deformation. This separation of voltage is performed by a bridge circuit. The PZT can be modeled as a voltage source (V_p) and capacitor (C_p) in series, resulting in a bridge circuit that is balanced with a capacitor of matched capacitance (C_m), as shown in Figure 1. The difficulty in balancing the bridge circuit is attributed to changes in the PZT's capacitance caused by temperature variations. Two types of PZT are considered in this study, 5H and 5A. The 5H piezoelectric shows a very significant temperature dependency, and 5A piezoelectric shows a lower sensitivity in comparison to 5H. However, the 5A piezoelectric still exhibits important temperature dependent characteristics[23]. For the 5A materials, it has been analytically estimated that every 5.5 °C change in temperature results in a one percent change in capacitance of the PZT patch (70 x 10 x 0.1 mm), as shown in Figure 2.

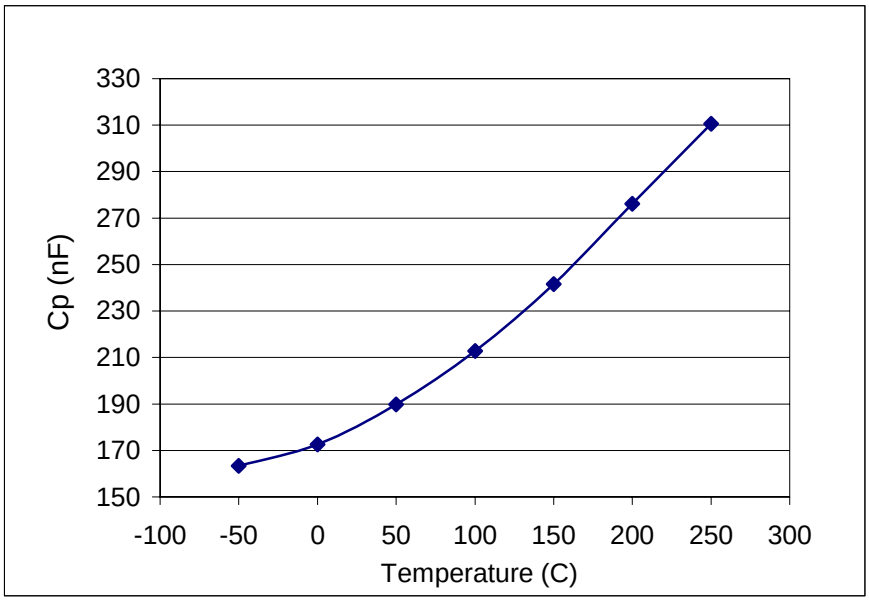

Figure 2: PZT Capacitance (5A, 70x10x0.1 mm) vs. Temperature

Analytical Model

In order to find a useful temperature range for the PZT 5A material, an analytical model of the self-sensing circuit, shown in Figure 1, was developed. The model consisted of an aluminum cantilever beam (.355 x.311 x.005 m) with two mounted PZT patches (70 x 10 x 0.1 mm). This structure will be discussed further in a later section. A self-sensing bridge circuit was constructed on a breadboard to allow for easy replacement of the matched capacitor during experimentation.

The first part of the analytical model consists of the derivation of the PZT sensing voltage (V_p) in response to the actuation, which is proportional to the strain field applied to the PZT. This can be calculated based upon piezoelectric constitutive and Euler-Bernoulli dynamic beam equations[24]. The second part of the model focuses on the dynamic characteristics of the bridge circuit which will be detailed in this section. The bridge circuit in Figure 1 can be simplified by replacing the components in the circuit with their equivalent impedances, as illustrated in the Figure 2. Once again, a PZT is modeled as a pure capacitor (C_p) in series with a voltage source

(V_p) which is caused by the actuation. Because both V_c (applied voltage) and V_p are considered as AC sources of unknown frequencies, one must divide the circuit into two parts by the principle of the superposition. After replacing the components in the circuit with their equivalent impedances, the circuit becomes a simplified voltage divider. In Figure 2, Z_p is the electrical impedance of PZT, Z_m is the electrical impedance of the matched capacitance, and Z_{eq} is the electrical impedance of the signal conditioning device. The sensor voltage is defined as the voltage difference between V_1 and V_2, as in equation (1), while V_1 is defined as the sum of V_{1c} and V_{1p}, shown in Figure 3:

$$V_s = V_1 - V_2 = V_{1c} - V_2 + V_{1p} \tag{1}$$

Using the voltage loop method in the Laplace domain and substituting the voltage terms with equivalent electrical impedances allows equation (1) can be rewritten as:

$$\begin{aligned} V_s &= \frac{Z_{eq}}{Z_{eq}+Z_p}V_c - \frac{Z_{eq}}{Z_{eq}+Z_m}V_c + \frac{Z_{eq}}{Z_{eq}+Z_p}V_p \\ &= \frac{C_p \cdot R_1 \cdot s}{R_1 \cdot s\left(C_1+C_p\right)+1}V_c - \frac{C_m \cdot R_1 \cdot s}{R_1 \cdot s\left(C_1+C_m\right)+1}V_c + \frac{C_p \cdot R_1 \cdot s}{R_1 \cdot s\left(C_1+C_{p\cdot}\right)+1}V_p \end{aligned} \tag{2}$$

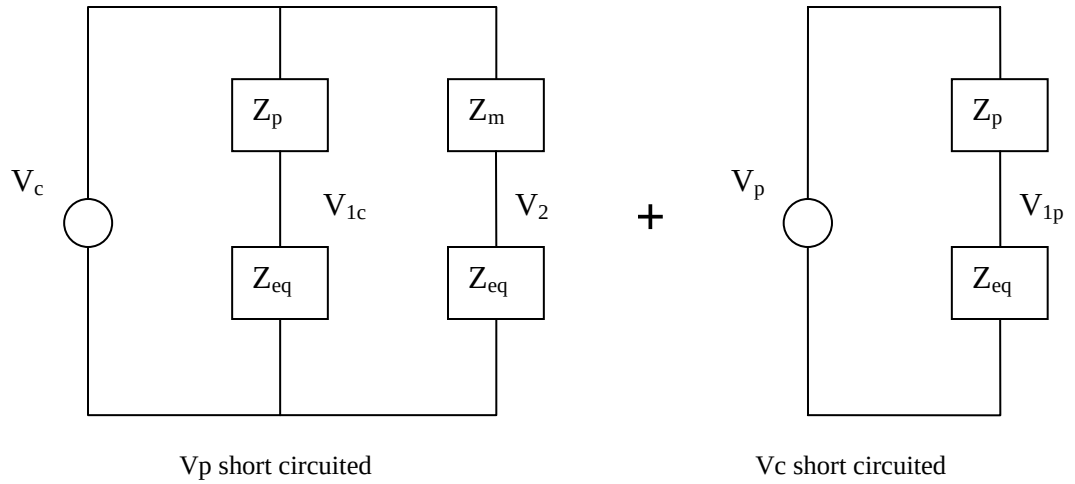

Figure 3: Simplified bridge circuit diagram

Equation (2) demonstrates when the value of C_P is equal to C_m, the bridge circuit is balanced and the resulting output voltage is proportional to the sensing voltage (V_P). If the bridge circuit is not balanced, a portion of V_C is superimposed with V_P, resulting in potential instability or loss of control effectiveness. Loss of stability would cause a very serious problem because Vc is usually a magnitude greater than that of V_P. This phenomenon of circuit unbalance has been observed in many cases[13].

Analytical Observations

Prior to collection of experimental data, analytical simulations were performed to study the reaction of the system to an unbalanced bridge circuit. With the positive position feedback (PPF) controller disconnected from the rest of the analytical model, frequency response functions (FRF) of the entire beam/circuit system were taken. The value for C_p was varied to observe the effect of the unbalanced bridge circuit on the FRFs.

With a variation in C_p, a change in resonant and anti-resonant locations in the FRF was observed. For values of C_p less than C_m, the anti-resonance appears before the resonance, and

the opposite occurs when C_p is greater than C_m, as shown in Figure 4. In addition, because the circuitry allows more of the control signal to appear in the sensor signal as the circuit becomes unbalanced, the magnitude of unmatched FRFs exhibit upward shifts compared to that of the balanced FRFs. With this observation, it is concluded that, by observing the FRF shapes, one can qualitatively assess the imbalance in the bridge circuit as well as whether the matched capacitance is greater or less than the capacitance of the PZT.

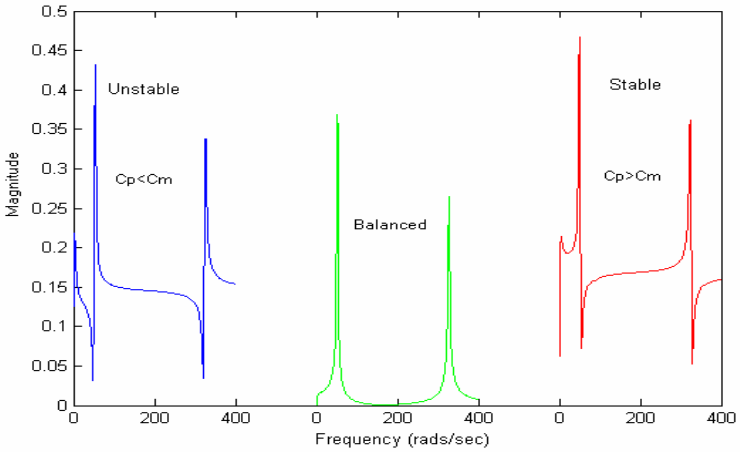

Once the pattern changes in FRF were identified, the stability of the system with PPF[25] control was investigated. It was expected that the reverse of the resonance and anti-resonance would indicate the stability of the system if the feedback controller was activated. The PPF controller was turned on after the gain and damping of the PPF was adjusted under the balanced circuit condition. When the resonance occurred before the anti-resonance, the analytical model became unstable with the activation of the PPF controller. When the anti-resonance occurred before the resonance, the system would remain stable and vibration reduction was still effective. However, when the value of C_p became increasingly smaller than C_m, the effectiveness of vibration control was decreased to the point where there was no apparent vibration reduction. Figure 5 demonstrates the relationship between C_P and C_m relative to control stability. It is apparent from these plots that the performance in vibration control deteriorates as the values of the PZT's capacitance changes. As the circuit becomes unbalanced, the control performance degrades because the circuit cannot fully cancel out the control signals, which begins to show up in the sensor responses.

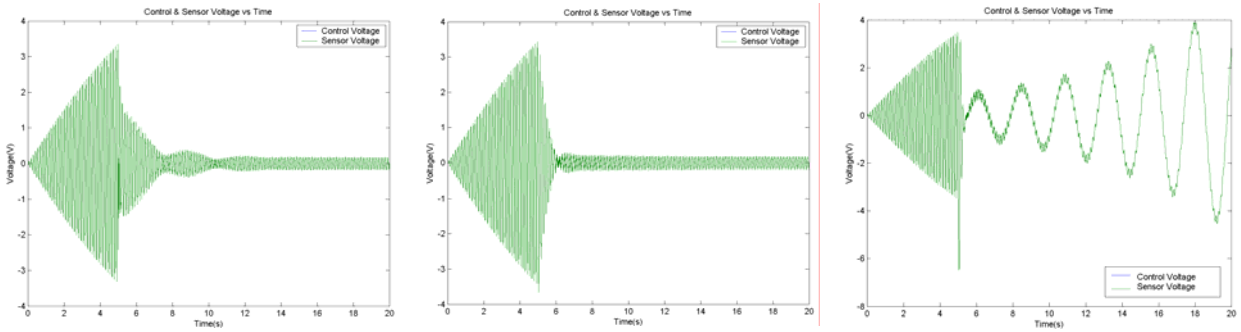

(a) $C_P=.9C_m$ (b) $C_P=C_m$ (c) $C_P=1.06C_m$

Figure 5: Effects of changes in Cp on PPF Control

To quantify the cause of the instability, a simple mechanical structure consisting of a two degree of freedom (DOF) 'self-sensing system' was constructed and a stability analysis was performed, as illustrated in Figure 6. A force, F_1, representing the control voltage (V_c) was applied to the first DOF and the response at the same location, X_1, which is analogous to the sensor voltage (V_p), was measured and analyzed. A virtual force VF_1, equivalent to the voltage across the matched capacitor was applied in the direction opposite to F_1. Therefore, if VF_1 and F_1 equal, each will cancel out and only X_1 can be measured, as in the self-sensing actuation. The mechanical equivalent system was used to better characterize the self-sensing system.

If F_1 is greater than VF_1, then the resultant output will be $X_1+\Delta F_1$ which represents the case where $C_p<C_m$. In positive feedback control, such as PPF, this case will create a stable system. However, in most "negative" feedback control systems, the resulting control will be unstable. The exact opposite occurs when F_1 is at a lesser value than VF_1 ($C_p>C_m$).

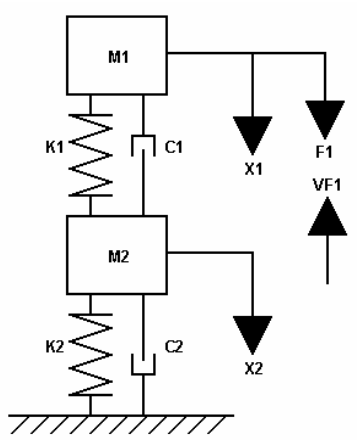

Figure 6: 2 DOF mechanical system equivalent to the Self-Sensing Circuit

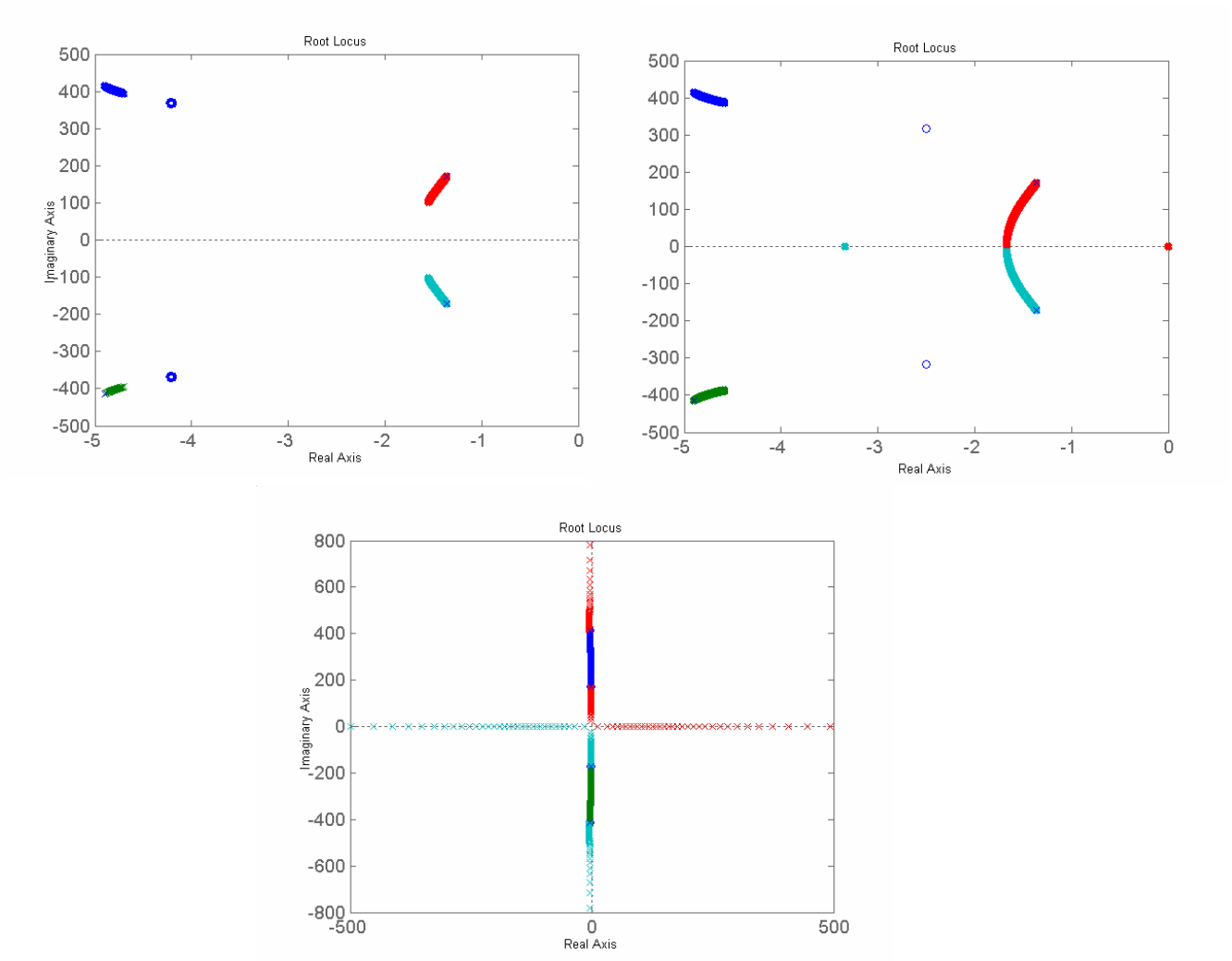

Figure 7: Root locus plots of the self-sensing system
a)C_p>Cm, b)C_p=C_m, c)C_p<C_m

Figure 7 illustrates the root locus plots, showing the stable case, perfect balance, and unstable case for the 2 DOF system. For the negative feedback control, the systems are stable under the conditions when $C_p > C_m$ and $C_p = C_m$. When $C_p < C_m$, the roots of the system cross over the right half plane, resulting in system instability. The conclusions reached from this analysis validate the results obtained from the analytical model. Once again, it should be noted that this analysis is valid for the negative feedback control. For a positive feedback control system, which is being considered in this study, the exact opposite would occur.

This analysis provides important design guidelines for the construction of self-sensing circuitry. For a positive feedback control system, the matched capacitance must be designed to have the same or higher value than the PZT capacitance in order to avoid possible instability of the system. For instance, if the system analyzed in this paper were operated in the temperature range 0-50 °C, a matched capacitance of 190 nF (refers Figure 2) will be unconditionally stable at all temperature ranges with PPF control systems. However, if temperature increases beyond 50 °C and reaches 60 °C, the system will go unstable.

INCREASING THE STABILITY OF THE SELF-SENSING CIRCUIT

Proposed Modifications

Once the dynamics of the self-sensing actuation were identified, the authors propose two modifications to the self-sensing circuit that potentially improve the stability of the system. Adding a capacitor in series or parallel with the PZT capacitance (C_p) and the matched capacitance (C_m) should increase the stability of the self-sensing circuit. Both modifications are based on the idea that adding capacitance to the circuit would change the equivalent capacitance in such a way that a temperature disturbance in the PZT patch would produce a smaller change in

the capacitance mismatching between C_p and C_m. The parallel and series connections were introduced in an attempt to change the total effective capacitance of the PZT and the matched capacitor in two different ways. For instance, the parallel connection increases the overall capacitance of the PZT/added capacitor combination, while the series connection decreases it.

A Theoretical Case for Adding Capacitors

A theoretical example is used to illustrate the effects of added capacitance. Assume that in a self-sensing circuit C_p and C_m are equal to 100 nF. It is also assumed that there is a temperature change that produces a 5 nF increase in the capacitance of C_p. In the case where there is no added capacitance, this change creates a 5% difference in matching between C_p and C_m. We also assume that a 5% mismatch leads to instability.

The theoretical circuit will now be modified by placing an added capacitor (C_{add}) of 100 nF in parallel with C_p and C_m. In this scenario, the 5 nF disturbance in C_p will not produce the same percentage mismatch between C_p and C_m because the parallel addition of C_{add} changes the equivalent capacitance (C_{eq}) according to Equation (3).

$$C_{eq} = C_{add} + C_p \tag{3}$$

A disturbance equivalent to the first example now only produces a 2.5% mismatch between C_p and C_m. A similar example can be arranged for the addition for C_{add} in series with C_p and C_m. The equivalent capacitance changes according to Equation (4) and the 5 nF temperature disturbance in C_p only creates 2.4% mismatch between C_p and C_m. Therefore, both of the modified circuits are stable even though they experience the same temperature induced change in C_p that drove the original system unstable. Figure 8 illustrates the proposed design scheme with 5 nF increase in capacitance of PZT (C_d).

$$C_{eq} = \frac{1}{\left(\left(1/C_{add}\right)+\left(1/C_{p}\right)\right)} \tag{4}$$

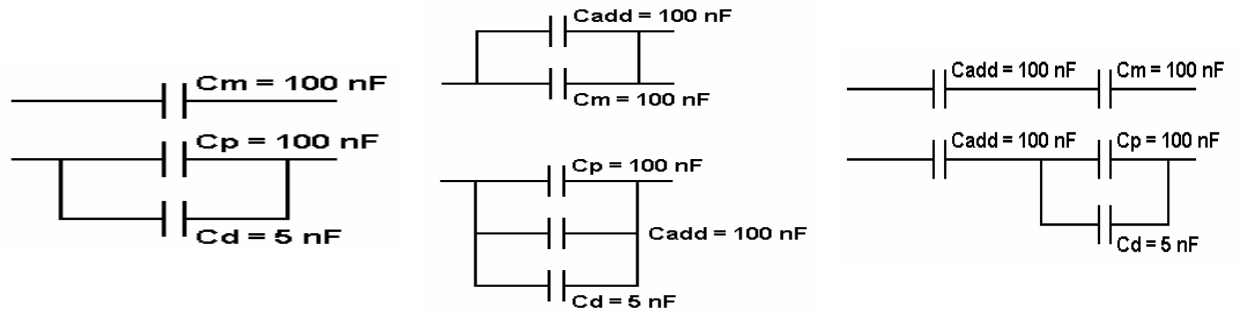

(a) No added capacitor. 5% mismatch

(b) Parallel added capacitor. 2.5% mismatch

(c) Series added capacitor. 2.4 % mismatch

Figure 8: Proposed self-sensing design scheme with added capacitor and disturbance

Analytical Modeling of Added Capacitance

The addition of series and parallel capacitors to the self-sensing circuit were modeled analytically because the previous scenarios are too oversimplified to account for the true effects of temperature changes on the circuit. Adding capacitance to the self-sensing circuit will change the circuit dynamics. Therefore, the transfer functions used within the Simulink® models had to be adjusted for this change in electrical impedance. Equation (5) shows the transfer function for the added series capacitor, in which C_{meq} refers the changes in the value of the matched capacitor as in the same manner in equation (3) and (4).

$$V_s = \frac{C_{eq}\cdot R_1 \cdot s}{R_1 \cdot s\left(C_1 + C_{eq}\right)+1}V_c - \frac{C_{meq}\cdot R_1 \cdot s}{R_1 \cdot s\left(C_1 + C_{meq}\right)+1}V_c + \frac{C_{eq}\cdot R_1 \cdot s}{R_1 \cdot s\left(C_1 + C_{eq}\right)+1}V_p \tag{5}$$

The PPF parameters were held constant for the analytical simulation as in the previous case. It should be noted, however, that the PPF parameters might have to be varied to alter

system performance during the experimental verification. The value of C_p was set equal to C_m with 170 nF (at 21.1 °C) to simulate an experiment at room temperature with PZT 5A material.

Analytical Results

The results of the analytical simulation in Figure 9 indicate that the added series and parallel capacitors significantly increase stability. With no added capacitance, the system was stable until C_p was 5% greater than C_m, and when C_p was 10% less than C_m. The settling time (t_s) of the original system was 1.25 s. A series added capacitor equal to the value of C_m remains stable until C_p was 15% greater than C_m, but when C_p was 10% less than C_m the settling time increased to 5.05 s. A parallel-added capacitor equal to C_m remained stable till C_p was 9% greater than C_m, and the settling time increased to 2.40 s when C_p was 10% less than C_m.

In the simulation, a 1% increase in C_p is equivalent to a 5.5 degree Celsius increase in temperature for PZT 5A materials. Thus, a parallel addition will increase stability for an additional 22 °C change in temperature, and a series addition will increase stability an additional 55 °C change in temperature. The downside is that the overall performance in vibration reduction is decreased as the series settling time increased by 304% and the parallel settling time increase by 92%. The gains remained constant for the experiment. As a result of the increase in stability, it would be possible in the experimental case to increase the gain, which would reduce the settling times. Thus, the trade-off would be increased stability at the cost of increased power to the actuator. From the figures, the magnitude of the sensing voltage with an added capacitor is slightly different from that of the original configuration. This is due to changes in the sensor's electrical impedance associated with the capacitance modification. For the parallel case, the sensor impedance is decreased thereby providing the improved signal to noise (SNR) ratio, and

the exact opposite occurs for the series connection. The differences are insignificant, therefore, no modification is made in the electronics setup to preserve the same SNR ratio.

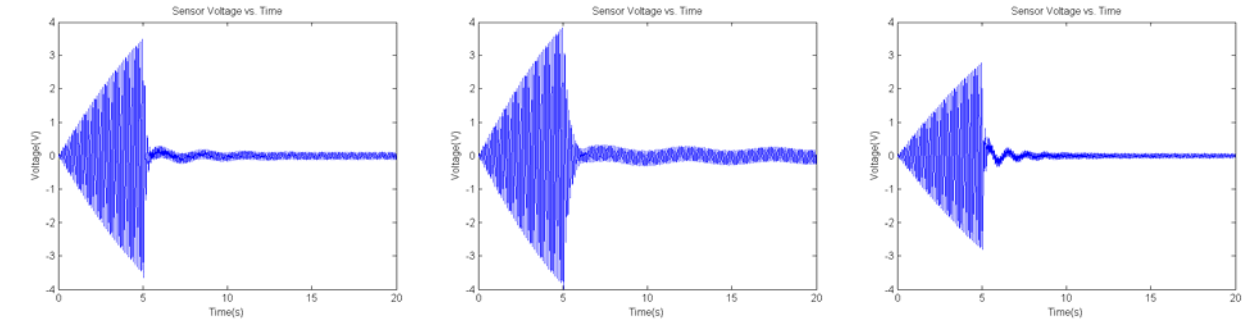

(a) No added capacitor at 5% (b) Parallel case at 9% (c) Series added case at 15%

Figure 9: Stability Thresholds for Three Cases

EXPERIMENTAL VERIFICATION

Once the effectiveness of the proposed design was analytically confirmed, the next task was to experimentally verify our theoretical findings. The test structure was an aluminum beam with a cantilever configuration.

Experimental Setup

An angle iron bracket was bolted to a square sheet of aluminum (.355 x.311 x.005 m) that served as the base of the structure. Two pieces of PZT 5A material were mounted to a cantilever beam clamped to the angle iron bracket, as shown in Figure 10. As a result of unexpected grounding issues, only the root patch was utilized during experimentation. Thus, the vibration disturbance and self-sensing actuation were handled with the one PZT patch at the root of the beam. Table 1 contains the important dimensions and specifications for the structure.

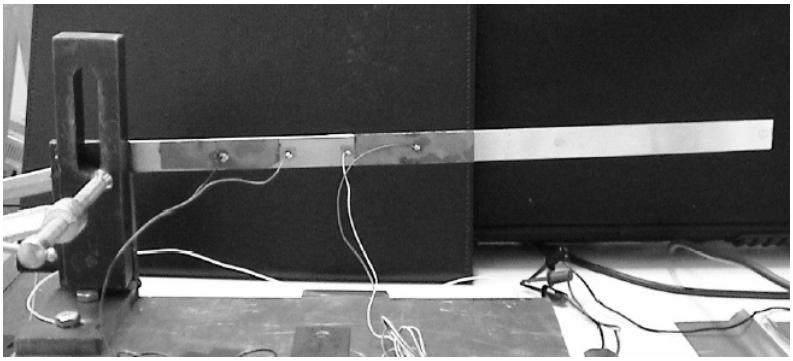

Figure 10: Test setup -Cantilever beam with PZT attached

Length	0.398m
Width	0.190m
Thickness	0.00158m
Distance from root to patch	0.0180m
Length of root patch	0.072
Distance between patches	0.045
Length of patch 2	0.072
E	6.90E+10
Base	0.335x0.311m
Base thickness	0.005

Table 1: Cantilever beam data

A self-sensing circuit was assembled on a circuit board, and the op-amps were powered by a Calex® dual source DC power supply. A Dactron® SPECTRABOOK® was used for data acquisition and to supply chirp and sine disturbance inputs to the structure. The PPF controller was built in Simulink® and implemented with a National Instruments® 2345 data acquisition board with an XPC Target® card. The control output was amplified by a PCB® 790 inverting amplifier and then routed to the self-sensing circuit. A diagram of the self-sensing system (without the structure) is illustrated in Figure 11.

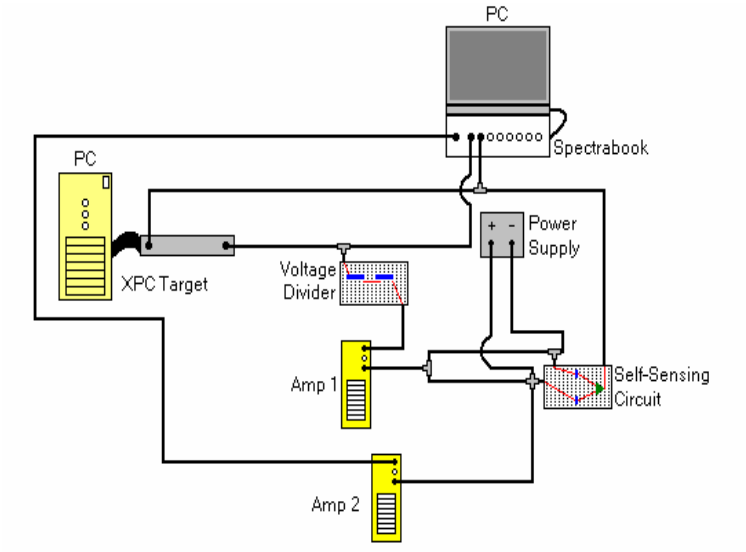

Figure 11: System diagram minus the structure

Experimental Results

Frequency response functions were measured for increasing and decreasing values of C_m. When C_m was less than C_p, the FRFs showed resonances occurring before anti-resonances. When C_m was greater than C_P, the exact opposite occurred, as shown in Figure 12. When the capacitances were matched, the anti-resonances were not seen in the FRF because the small magnitudes could only be seen by using a semi-log scale. The resonant/anti-resonant patterns seen in the experimental FRFs match those predicted by the analytical studies. The magnitude shifts in the FRF predicted by the analytical model were also observed in the experiments. When $Cp \neq Cm$, a portion of the applied voltage is mixed with sensing voltage and this caused the shifts in the magnitude described in the analytical section. Once again, the results confirm that one can qualitatively assess the condition of the bridge circuit by observing the shape of frequency response functions.

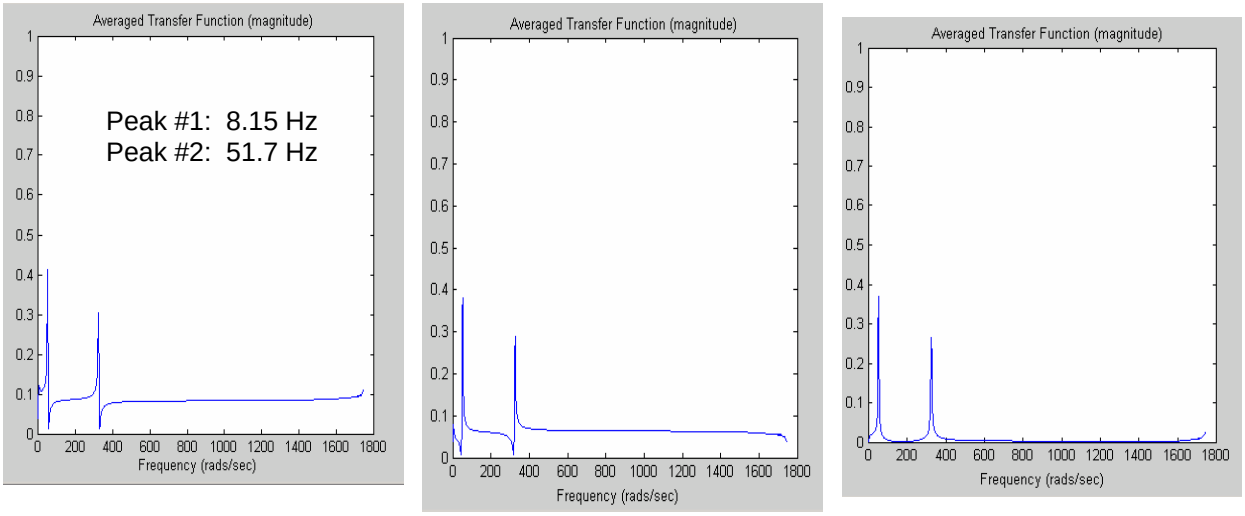

(a) C_p is 29% greater than C_m (Unstable Case)

(b) C_p is 34% less than C_m (Stable Case)

(c) Cp = Cm (Balanced Case)

Figure 12: Experimental Frequency Response Functions

After the FRF data was collected, the values of C_p and C_m were measured, and adjustments were made to ensure perfect matching. All additional capacitors added (C_{add}) to the system were equal to C_p at 21.1 °C. Experimentally, the value of the PZT capacitance was identified as 100 nF. All PPF parameters were held constant during the entire testing. The system was tested in the matched case for the following conditions: no added capacitor, a series added capacitor, and a parallel added capacitor. All three systems were tested with no capacitance disturbance caused by a temperature change. Figure 13 shows that, with no disturbance, the no-added, series-added, and parallel-added capacitor cases were all stable. Note that the results are not plotted on the same magnitude scale. With the added capacitor, the sensing voltage is decreased with the increase in equivalent capacitance of the PZT. In addition, the overall vibration reduction performance is somewhat decreased. Without the added capacitor, the reduction was achieved up to 95%. With added capacitors, the achieved vibration reductions were only 70%.

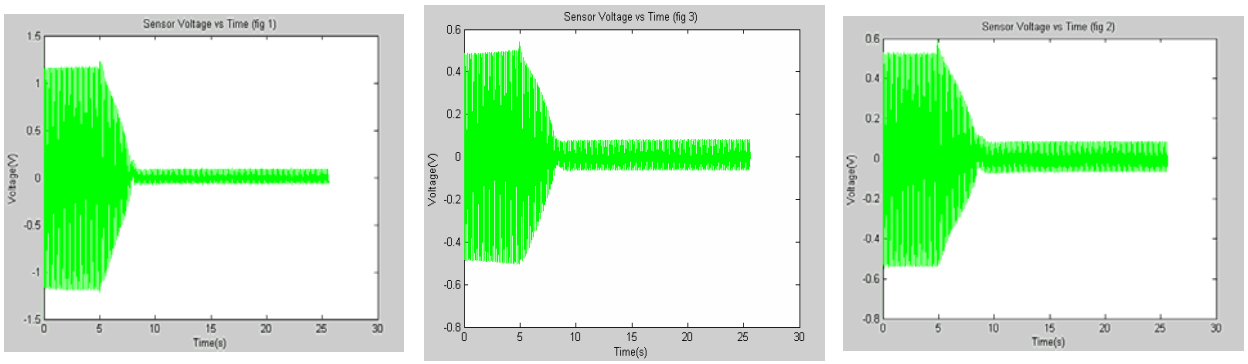

(a) No added capacitors (b) Series added capacitors (c) Parallel added capacitors

Figure 13: Sensor voltage vs time for no temperature disturbance

A second group of tests were conducted for a simulated temperature change. A simulated temperature change was experimentally tested by adding a 4 nF capacitor in parallel with the PZT. Figure 14 shows the results of the tests when the 4 nF disturbance was added to the C_p. The no-added capacitor case was unstable, but the series and parallel added capacitor cases still remained stable, although they show more pronounced decreases in performance in both settling time and steady-state responses. It should be noted that the input and output voltage of XPC card is limited to only ten volts, so a saturation block was employed in the Simulink® code to protect the XPC card from potential overload. Therefore, unstable case ((a) in figure 14) does not produce the unbounded output seen in the analytical simulation cases. Instead, the unstable system experiences beating and never reduces to a stable case because the controller continues to perturb the system due to imbalances in the self-sensing bridge.

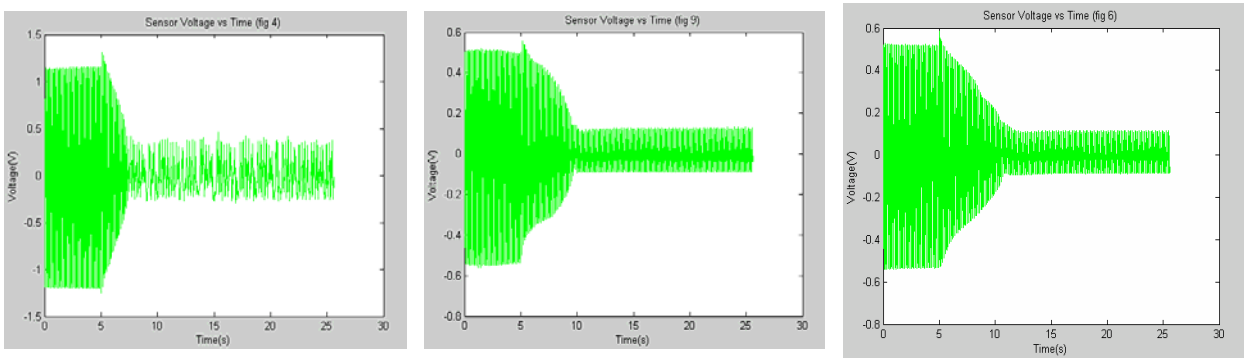

(a) No added capacitors (b) Series added capacitors (c) Parallel added capacitors

Figure 14: Sensor voltage vs time for a 4nF disturbance caused by a temperature change

A third series of tests were conducted to simulate an even larger temperature change. A 10 nF disturbance was added to the circuit in various configurations to simulate a large temperature change. This corresponds to changes in temperature up to 50 °C for the experimental configuration. Figure 15 shows the results of these tests when the disturbance was added to C_p. In this case, only the circuit with the parallel added capacitance was still stable.

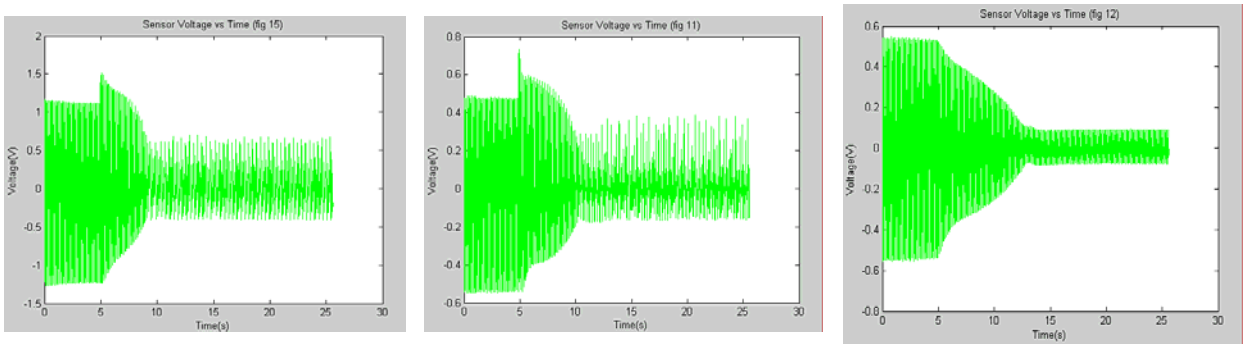

(a) No added capacitors (b) Series added capacitors (c) Parallel added capacitors

Figure 15: Sensor voltage versus time for a 10nF disturbance caused by a temperature change

The experimental tests clearly show that adding series and parallel capacitances to the self-sensing circuit can increase stability. The results also show that adding capacitors increases the settling time and decreases the effectiveness of vibration control (see Table 2). This result

occurs because the capacitors absorb energy like springs in mechanical systems, which thus decreases the sensing and applied voltages.

It should be noted that the experiments performed in this analysis do not fully account for the power consumption requirement on each configuration. Energy requirements are an important design factors in structural control applications. Average power, peak power required and total energy consumed directly influence the performance of the overall system. The average power requirement for piezoelectric capacitive loading can be readily derived from lumped equivalent circuits as,

$$P = 2\pi f C V_{rms}^{\ 2} \qquad (6)$$

Where P is the average power requirement, f is frequency, C is the capacitance, and V_{rms} is the RMS of the applied voltage. In the parallel connection, this method would inevitably decrease the power utilization by increasing the effective capacitance (C in Equation (6)) of the PZT. On the other hand, for the series connection, it may require less power by decreasing the effective capacitance of the PZT, however, the electronics used in sensing devices, such as charge amplifiers or voltage followers, need to be redesigned in order to accommodate changes in the sensor impedances and to provide a better signal to noise ratio. The experimental results in the Figures 13, 14, and 15 show the effects associated with the changes in PZT capacitance.

A final experimental test was conducted for the parallel case in an attempt to increase effectiveness while retaining increased stability. The power used for the PZT control actuation was increased by a factor of two. Figure 16 shows the settling time decreased from 7.70 s to 2.03 s when a 12 nF disturbance was added in parallel to $C_{p,}$ and the system remains stable. This

concludes that there is a tradeoff between increased stability and effectiveness. In order to maintain the effectiveness, one should provide increased power to the controller.

Table 2: Experimental results

	Stable Condition	Settling Time (s)
Cp=Cm w no Cadd	yes	2.81
Cp=Cm w Series Cadd	yes	3.46
Cp=Cm w Parallel Cadd	yes	3.35
Cp=Cm wo Cadd+4 Nf	no	N/A
Cp=Cm w Series Cadd+4 nF	yes	6.08
Cp=Cm w Parallel Cadd + 4 nF	yes	5.03
Cp=Cm wo Cadd+10 nF	no	N/A
Cp=Cm w Series Cadd+10 nF	no	N/A
Cp=Cm w Parallel Cadd + 10 nF	yes	7.70

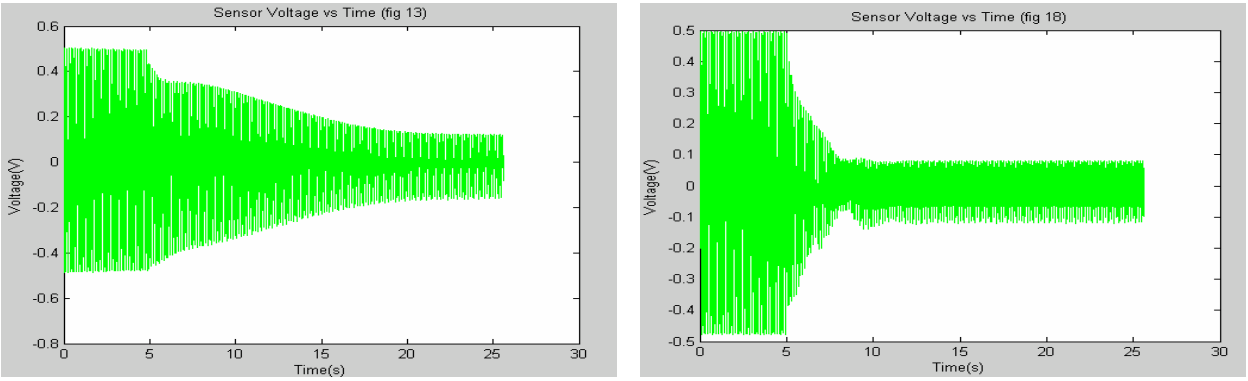

(a) Original controller (b) Increased power (by two) controller

Figure 16: Vibration reduction increases as the power to the controller increases

In summary, the experiments conclusively show that the proposed design scheme increase the stability of the self-sensing system. The improved stability comes at the cost of the reduction in vibration control performance or the increase in power required for the control system.

DISCUSSION

No-added capacitance

This study has focused on identifying the usable temperature range of the 5A piezoelectric material. A cantilever beam structure using PZT as a self-sensing actuator was constructed. An analytical model of the self-sensing actuation system was created using MATLAB® Simulink®. The results from this analytical model (with no-added capacitor) show that an increase in C_p by 4% or 22 °C from room temperature will continue to allow for effective vibration control. In analytical model observations, the positive position feedback controller could not create a stable system if C_p was equal to or exceeded a 5% increase from room temperature capacitance. Experimentally, with no added capacitance, when C_p was increased 4.19% (4nF) the system went unstable.

Parallel-added capacitance

The analytical model was modified to facilitate a capacitor placed in parallel with the PZT and the matched capacitance. The analytical model predicted that the system would remain stable up to the point where C_p exceeded C_m by 9%. When C_p was 10% greater than C_m the system went unstable. In the experimental case, when C_p was increased by 10.5 % (10 nF) beyond C_m the system remained stable. This result indicates that the system will remain stable for an increase of 35 °C beyond the point where the system with no added parallel capacitor went unstable.

Series-added capacitance

The analytical model was also modified to facilitate a capacitor placed in series with C_p and C_m. An increase in stability was also observed. A 13 % increase in PZT capacitance beyond room temperature was a result of the added series capacitor while still allowing for stable

vibration reduction. These tests were performed to show increased stability over the case with no added capacitors. The series capacitor stabilized the 4.19% (4 nF) increase in C_p, as did the parallel capacitor, but was unable to fully control the 10.5% (10nF) increase.

Settling time

The downside of adding capacitance in series and parallel seems to the effect on settling time when C_m is greater than C_p (a stable case that causes the controller to be ineffective in vibration reduction). When a capacitor is added in parallel or in series to C_p and C_m, the applied voltage drops. The reduction in the applied signal causes the system to damp out vibrations more slowly. In the experimental case, this increase in settling time could be offset by increasing the power to the PPF. There is potentially a tradeoff between stability and effectiveness that could be optimized based on the amount of reduction desired and the change in temperature the system will experience.

Several Issues

A critical aspect of sensing signals from the self-sensing circuit is that the sensing voltage could inaccurately identify actual setting time or amount of vibration suppression if the circuit is not balanced. A more accurate method to show the structure before and after control would be to use a separate sensor to present the effectiveness of the control strategy. In this study, only the self-sensing signals were analyzed to assess the performance of the proposed concept. Therefore, a more detailed analysis needs to be carried out using a separate sensor to truly characterize the dynamic behavior of the proposed self-sensing circuitry, along with the thorough investigations in the efficiency of power utilization and improvement of SNR with the changes in effective capacitance of the PZT.

It should be noted that, in this study, only the temperature variations associated with the environmental condition changes were considered. The temperature of PZT also changes as a function of PZT duty cycle by simply being in the control loop, resulting in changes in the capacitance of PZT. The understanding of this effect is beyond the scope of this study and will be investigated along with other issues to improve the performance of the proposed self-sensing concept.

CONCLUSIONS

The dynamic characteristics of self-sensing actuation are quantitatively studied for the first time in literature. Two new design schemes (adding capacitors in series or parallel to the traditional bridge circuit) are used to increase control stability, which makes self-sensing actuation more commercially viable. The effectiveness of the two design schemes is enhanced at the cost of increased power to the controller. Both new design schemes are validated experimentally and shown to improve system performance with respect to temperature changes.

Further study in optimizing the use of series and parallel capacitors is necessary to create a more robust system. This resulting system should allow for a large range of PZT capacitances caused by temperature changes while still allowing for optimal vibration reduction. In addition, these techniques for self-sensing robustness can be extended to complex and real-scaled structures where damage detection is warranted. A single piece of piezoelectric materials can simultaneously detect damage and control structures[26], yet up to this point instability has limited the usefulness of PZT in these applications. A more robust self-sensing circuit could make PZT as a self-sensing actuator more viable for detecting damage and controlling complex structures at the same time.

ACKNOWLEDGEMENTS

The research was conducted at the Los Alamos National Laboratory in Los Alamos, NM, as a part of the 2003 Dynamics Summer School. The Engineering Sciences and Applications Division and The Department of Energy's Education Programs Office provided funding for this research. Great thanks go to the following companies for their software donations: MathWorks Inc. (MATLAB®), and Vibrant Technology Inc. (ME'ScopeVES®). The authors would like to acknowledge Mr. Henry Sodano from Virginia Tech for his expert advice in the construction and troubleshooting of the experimental self-sensing bridge circuit. The authors would also like to give great thanks to Dr. Charles Farrar for organizing the Dynamic Summer School.

REFERENCES

[1] Dosch J.J., Inman D.J., Garcia E., "A Self-Sensing Piezoelectric Actuator for Collocated Control" Journal of Intelligent Material Systems and Structures, Vol. 3, pp. 166-185, 1992.

[2] Goh, C. J., Caughey, T. K., "On the Stability Problem Caused by Finite Actuator Dynamics in the Control of Large Space Structures", International Journal of Control, Vol. 41 No. 3, pp. 787-802, 1985

[3] Tzou, H.S., Hollkman, J.J., "Collocated Independent Modal Control with Self-Sensing Orthogonal Piezoelectric Actuators (Theory and Experiment)," Smart Materials and Structures, Vol 3, pp. 147-156, 1994.

[4] Frampton, K.D., Clark, R.L. and Dowell, E.H., "Active Control of Panel Flutter with Linearized Potential Flow Aerodynamics," AIAA Paper No. 95-1079, Proceeding of the 36th AIAA/ASME/ASCE/AHS/ASC Structures, Structural Dynamics and Materials Conference, April 10-13th, New Orleans, LA, pp. 2273-2280, 1995.

[5] Dongi, F., Dinkler, D. and Kroplin, B., "Active Panel Flutter Suppression using Self- Sensing Piezoactuators," AIAA Paper No. 95-1078, Proceeding of the 36th AIAA/ASME/ASCE/AHS/ASC Structures, Structural Dynamics and Materials Conference, April 10-13th, New Orleans, LA, pp. 2264-2272, 1995.

[6] Vallone, P., "High-performance Piezo-based Self-sensor for structural Vibration Control," Proceedings of 2nd SPIE Smart Structures and Materials Conference, Newport Beach, CA, Vol. 2443, pp. 643-655, 1995

[7] Ko, B., Tongue, B.H., "Acoustic Control using a Self-sensing Actuator," Journal of Sound and Vibration, Vol. 187, pp. 145-165, 1995.

[8] Leo, D.J., Limpert, D. "A Self-sensing Technique for Active Acoustic Attenuation," Journal of Sound and Vibration, Vol. 235, No. 5, pp. 863-873, 2000.

[9] Pardo de Vera, C.; Guemes, J. A., "Embedded self-sensing piezoelectric for damage detection," Journal of Intelligent Material Systems and Structures, v.9, no.11, 876-882, 1999.

[10] Vipperman, J.S., "Simultaneous Qualitative Health Monitoring and Adaptive Piezoelectric Sensoriactuation," AIAA Journal, Vol. 39, No. 9, 1822-1825, 2001.

[11] Jones, L., Garcia, E., Waites, H., "Self-sensing Control as applied to a Stacked PZT actuator used as a micropositioner," Smart Materials and Structures, Vol.3, pp. 147-156, 1994.

[12] Sodano, H.A., Park, G., Inman, D. J., "An Investigation into the Performance of Macro-Fiber composites for Sensing and Structural Vibration Applications," Mechanical Systems and Signal Processing, Vol. 18, No. 3 pp. 683-697.

[13] Tani J., Cheng G., Qiu J., "Effectiveness and Limits of Self-Sensing Piezoelectric Actuators" Proceedings of 1st Structural Health Monitoring Workshop, Stanford, CA, pp. 503-514, 1997.

[14] Cole, D.G., Clark, R.L., "Adaptive Compensation of Piezoelectric Sensoriactuators," Journal of Intelligent Materials Systems and Structures, Vol. 5, pp. 665-672, 1994.

[15] Vipperman, J., Clark, R.L., "Implementation of an Adaptive Piezoelectric Sensoriactuator," AIAA Journal, Vol. 34, pp.2102-2109, 1996

[16] Oshima, K., Takigami, T., Hayakawa, Y. "Robust Vibration control of a Cantilever Beam using Self-sensing Actuator," JSME International Journal, Series C. Vol. 40, No. 4, pp. 681-687.

[17] Spangler, R.L., Hall, S.R. "Broadband Active Structural Damping using Positive Real Compensation and Piezoelectric Simultaneous Sensing and Actuation," Smart Materials and Structures, Vol. 3, pp. 448-458, 1994.

[18] Jones, L.D., Garcia, E., "Novel Approach to Self-sensing Actuation," Proceedings of SPIE, Vol. 3041, pp. 305-314, 1997.

[19] Dong, W, Sun B., "Study on Observer based Piezoelectric self-sensing actuator," Proceedings of SPIE, Vol. 4414, pp. 472-475, 2001.

[20] Tonoli, A., Oliva, S., Caraelli, S., Civera, P., "Charge Driven Piezoelectric Transducers in Self-sensing Configuration," Proceedings of 7th SPIE Smart Structures and Materials Conference, Newport Beach, CA, Vol. 4327, pp. 743-752, 2001

[21] Okugawa, M., Sasaki, M., "System Identification and Controller Design of a Self-sensing Piezoelectric Cantilever Structure," Journal of Intelligent Material Systems and Structures, Vol. 13, pp.241-252, 2002.

[22] Nishigaki, T., Endo, M., "A Self-sensing Actuator using Piezoelectric Films with Different Thickness for Vibration Control of Curved Structures (Proposition of Principal Concepts and Applications to Cantilever and Circular Ring)," Proceedings of 11th International Conference on Adaptive Structures and Technologies, Japan, pp. 1-8.

[23] Piezo Systems, Inc,. (http://www.piezo.com)

[24] Poh, S. and Baz, A., "Active Control of a Flexible Structure Using a Modal Positive Position Feedback Controller," Journal of Intelligent Material Systems and Structures, Vol. 1, pp. 273-288, 1990.

[25] Fanson, J.L. and Caughey, T.K., "Positive position feedback control for large space structures", in Proceedings of 28th AIAA Structures, Structural Dynamics and Materials Conference, Monterey, CA, pp. 588-598,1987

[26] Inman, D.J., Ahmadia, M., and Claus, R.O., "Simultaneous Active Damping and Health Monitoring of Aircraft Panels," Journal of Intelligent Material Systems and Structures, Vol. 12, pp. 775-783